

## Measurement of heat capacity and enthalpy of formation of nickel silicide using nanocalorimetry

Ravi K. Kumamuru,<sup>1,2</sup> Lito De La Rama,<sup>1</sup> Liang Hu,<sup>1</sup> Mark D. Vaudin,<sup>2</sup> Mikhail Y. Efremov,<sup>1</sup> Martin L. Green,<sup>2</sup> David A. LaVan,<sup>2</sup> and Leslie H. Allen<sup>1,a)</sup>

<sup>1</sup>Department of Material Science and Engineering, University of Illinois at Urbana-Champaign, Illinois 61801, USA

<sup>2</sup>Ceramics Division, Materials Science and Engineering Laboratory, National Institute of Standards and Technology, Gaithersburg, Maryland 20899, USA

(Received 10 August 2009; accepted 6 October 2009; published online 5 November 2009)

The total enthalpy of reaction and heat capacity to 850 °C were measured using differential scanning nanocalorimetry (nano-DSC) for the reaction of a nickel and silicon bilayer at heating rates up to 10<sup>6</sup> K/s. Exothermic dips in heat capacity attributed to nickel silicide formation were found along with indications of phase changes at 430 and 550 °C. The postreaction phases were identified using electron backscattered diffraction. Samples with a Ni:Si molar ratio of 1.2 heated to 850 °C were a mixture of orthorhombic NiSi and the  $\theta$ -phase (hexagonal—Ni<sub>2</sub>Si); samples heated to 790 °C resulted in predominantly NiSi. © 2009 American Institute of Physics.

[doi:10.1063/1.3255009]

Nickel silicides are used as contact and potential gate materials in advanced complementary metal-oxide semiconductor devices. Nickel (Ni) forms a number of phases with silicon (Si). Ni–Si reactions have been studied with x-ray diffraction,<sup>1–4</sup> transmission electron microscopy,<sup>5,6</sup> Raman<sup>7</sup> and Auger-electron spectroscopy,<sup>3,8</sup> Rutherford backscattering (RBS),<sup>9</sup> and electron back-scattered diffraction (EBSD).<sup>10,11</sup> However, none of these techniques can quantitatively measure energetics of reactions.

Differential scanning nanocalorimetry (nano-DSC) was used to investigate Ni–Si reactions by measuring the heat capacity (Cp) of thin films using a silicon nitride (SiN<sub>x</sub>) membrane sensor with a platinum (Pt) strip used as both a heater and temperature sensor;<sup>12</sup> this technique has been used on a number of materials such as nanoparticles,<sup>13</sup> polymers,<sup>14</sup> and metal thin films,<sup>15,16</sup> but the temperature for quantitative measurements has been below 500 °C. Higher temperature measurements are challenging due to instability of the sensor temperature coefficient of resistivity (TCR) possibly due to stress induced voiding, electromigration, and alloying of Pt (50 nm) with the Ti adhesion layer ( $\approx$ 3 nm).<sup>17</sup> Calibration of the sensor is performed in a vacuum furnace; calibration at high temperatures is difficult due to current leakage and shunting through the substrate.

Instability in the sensor TCR is reduced by annealing the platinum resistor/sensor to  $\approx$ 850 °C. The TCR of the platinum strip was then calibrated in a vacuum furnace to 400 °C. A fourth order polynomial, the Callendar–Van Dusen (CVD) equation, for TCR in Pt was used to extrapolate the calibration up to 850 °C.

Investigation of the reaction between Ni and Si poses challenges. First, since the reaction is irreversible, averaging cannot be used to reduce noise. Second, both Ni and Si oxidize in air. Third, lattice rearrangement of the as-deposited Si and Ni films could occur as the temperature is raised. Any energy associated with it would interfere with the enthalpy measurement in the first pulse. For this purpose, *in situ* an-

nealing steps were performed after depositing each film.

The sample remained under vacuum in the electron-beam evaporator through the deposition and measurement in order to prevent oxidation of Ni and Si. A shadow mask<sup>18</sup> was used to restrict deposition to the active area of the sensor. A sensor with no sample was used as a reference. Base pressure during evaporation was  $5 \times 10^{-5}$  Pa; all measurements were performed at pressures below  $7 \times 10^{-5}$  Pa. Using the measured Cp and bulk values for density and specific heat, the sample contained 5.6 nmol of silicon, equivalent to a thickness of 25 nm; and 6.7 nmol of nickel, equivalent to a thickness of 17 nm (molar ratio Ni/Si=1.2). The grain size of the reaction products is large at tens of micrometers. RBS thickness measurements on a control silicon wafer with 66 nm of gold (to separate the substrate RBS signal from the deposited Si) gave thicknesses of 27 nm for Si and 16 nm for Ni, in close agreement with the Cp-based thickness measurements.

The experiments consist of the following stages—(a) Cp measurement before evaporation (to establish a baseline), (b) Si deposition, (c) annealing Si by applying current pulses (heating to  $\sim$ 800 °C), (d) Cp measurement after Si deposition, (e) Ni Deposition, (f) annealing and Cp measurement up to 150 °C after Ni deposition, (g) final Ni–Si reaction—initiated by heating sample while measuring Cp, and (h) additional heating cycles to confirm the completion of reaction, and to measure the Cp of the end products. For each Cp measurement [except the final Ni–Si reaction (g)], the sample was heated at four different heating rates, by varying the applied current. This data was used to correct for heat losses.<sup>12</sup>

EBSD in a scanning electron microscope (SEM) at 30 kV was used to identify the reaction products. Digital images ( $672 \times 512$  pixel<sup>2</sup>) were recorded and EBSD patterns were indexed using HKL FLAMENCO software using patterns from the PDF database which identified NiSi (PDF 38–0844, orthorhombic,  $a=0.523$  nm,  $b=0.566$  nm,  $c=0.326$  nm) and  $\theta$ -Ni<sub>2</sub>Si (PDF 65–1931, hexagonal,  $\theta$ -nickel-silicide,  $a=0.3805$  nm,  $c=0.489$  nm).

<sup>a)</sup>Electronic mail: l-allen9@uiuc.edu.

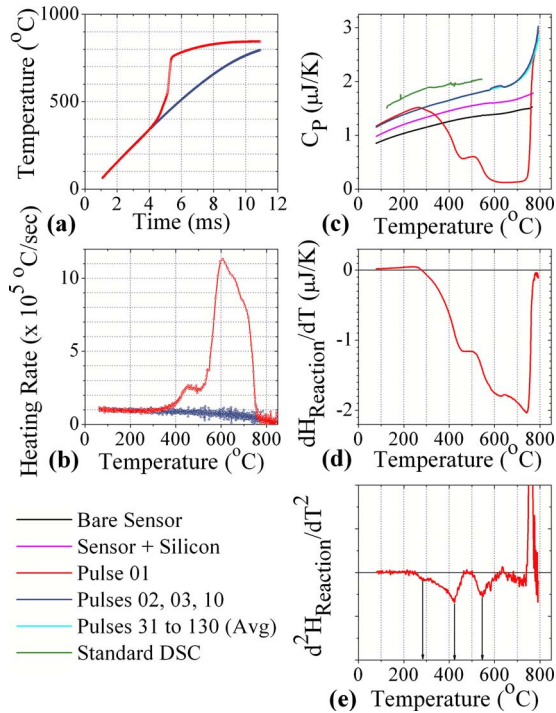


FIG. 1. (Color online) (a) Temperature profile. (b) Heating rate. (c) Heat capacities of the sensor and film at various stages of the experiment after accounting for heat loss. The top green line (Standard DSC) is from a conventional DSC (scan rate: 20 °C/min). Due to the small sample volume, the conventional DSC measurement is considered as arbitrary units for qualitative comparison; (b) the reaction peak— $dH_R/dT \approx C_{p,pulse01} - C_{p,pulse02}$ . (e) Derivative of the peak which shows three distinct inflection points.

Figure 1 shows the experimental data. An exothermic reaction is seen in the first 10 ms pulse, characterized by a sharp rise in the heating rate between 300 and 750 °C [Fig. 1(b)]. Subsequent pulses do not show this peak indicating that the reaction was completed.

The enthalpy of reaction ( $H_R$ ) was calculated by isolating the exothermic peak in the first cycle by subtracting heat capacity of the first cycle from the second cycle as derived below:

$$V_S I_S(t) = C_{p,PFilm} \frac{dT_S(t)}{dt} + C_{p,PSensor} \frac{dT_S(t)}{dt} + \frac{dH_R(t)}{dt} + P_L(t),$$

$$C_{p,Pulse01} \frac{dT_S(t)}{dt} = C_{p,PFilm} \frac{dT_S(t)}{dt} + C_{p,PSensor} \frac{dT_S(t)}{dt} + \frac{dH_R(t)}{dt},$$

$$\frac{dH_R(T)}{dT_S} = C_{p,Pulse01}(T) - C_{p,Tot}(T) \approx C_{p,Pulse01}(T) - C_{p,Pulse02}(T),$$

where  $T_S$  is sample temperature,  $C_{p,Pulse\#}$  is the  $C_p$  as shown in Fig. 1(c),  $C_{p,Tot}$  is the heat capacity of the sensor and deposited films which in pulse 01 changes from the  $C_p$  of the unreacted components to that of end products;  $P_L$  is the rate of heat loss due to conduction. Figure 1(d) shows the negative peak ( $dH_R/dT_S$ ). This peak shape with an abrupt drop beyond 700 °C is typical for experiments with various Ni

and Si molar ratios, indicating that the reaction stops quickly once all the silicon is consumed. By integrating this peak with respect to sample temperature, and referring the result (570 μJ) to the standard temperature 298 K (using data from Ref. 19), we estimate the enthalpy of the complete reaction, which is found to be -565 μJ. The average enthalpy per mole of atoms of Ni and Si deposited is -46 kJ. For comparison, the published heats of formation of NiSi and  $\delta$ -Ni<sub>2</sub>Si (orthorhombic) are -42.4 and -46.9 kJ per mole of atoms, respectively.<sup>20</sup> The value for  $\delta$ -Ni<sub>2</sub>Si is reported for comparison, as no value for  $\theta$ -Ni<sub>2</sub>Si was found in the literature.

Accuracy of the heat of formation measurements depends on error due to (1) noise ( $< \pm 1\%$ ), (2) temperature deviation from the CVD equation. Using aluminum melting point as a reference we estimate this to be  $\pm 9\%$ , which leads to a  $\pm 9\%$  uncertainty in  $H_R$  assuming a uniformly distributed error, but could be larger if temperature error is concentrated at high temperatures, (3) temperature variation due to sample misalignment, which is calculated to be about 1% for the sensor and shadow mask designs used. We estimate the total uncertainty in our current  $H_R$  measurements to be below  $\pm 10\%$ .

Nickel and silicon go through a number of reactions between 300 and 800 °C.<sup>1</sup> *In situ* x-ray diffraction<sup>1</sup> measurements during Ni-Si reactions for films with a similar molar ratio formed Ni<sub>2</sub>Si from 300 to about 500 °C, and NiSi was found from 500 up to 700 °C. We see a clear signature of distinct reactions at different temperatures in our measurements as variations in the heating rate [Fig. 1(b)]. The derivative of the exothermic region ( $d^2H/dT^2$ ) shows three negative peaks at 280, 430, and 550 °C [Fig. 1(e)]. The position of the 430 °C peak and the 550 °C peak coincide well with observations<sup>1</sup> of Ni<sub>2</sub>Si and NiSi, and another at 280 °C which may correspond to their unidentified phase.<sup>1</sup>

Sixty EBSD patterns collected along a line were manually indexed. A mixture of NiSi and  $\theta$ -Ni<sub>2</sub>Si was found. 48 of the 60 patterns could be indexed. Of those, 28 were found to be NiSi and 20 were  $\theta$ -Ni<sub>2</sub>Si. Figures 2(a) and 2(b) shows typical indexed EBSD patterns.<sup>21</sup> Ni<sub>2</sub>Si is reportedly stable above 825 °C and has also been found in co-sputtered Ni-Si mixtures quenched at around 420 °C.<sup>11</sup> Our samples reached 850 °C and cooled rapidly.

To understand the role of peak temperature in Ni<sub>2</sub>Si evolution an identical sample was heated to just 790 °C. Of the EBSD patterns that could be indexed, only one was  $\theta$ -Ni<sub>2</sub>Si while all the others matched NiSi [Fig. 2(d)]. A key difference between our measurements and those of others<sup>11</sup> is our much higher heating rate, which suggests that reaction kinetics have an influence on the final reaction products. Figures 2(e) and 2(f) show the grain structure of the reaction products after the complete Ni-Si reaction ( $> 800$  °C).

In conclusion, we have performed *in situ* nanocalorimetric measurements of heat capacity and enthalpy of Ni-Si thin film interfacial reactions. The reaction between the nickel and silicon films proceeded to completion in a single 10 ms experiment. Several phase changes/reactions were seen in the heat capacity measurements during the first heating cycle. Samples that remained below 800 °C were found to result in predominantly NiSi, while samples heated to 850 °C formed  $\theta$ -Ni<sub>2</sub>Si.

Nano-DSC (nanocalorimetry) can be effectively used to understand the energetics of thin film and interfacial reac-

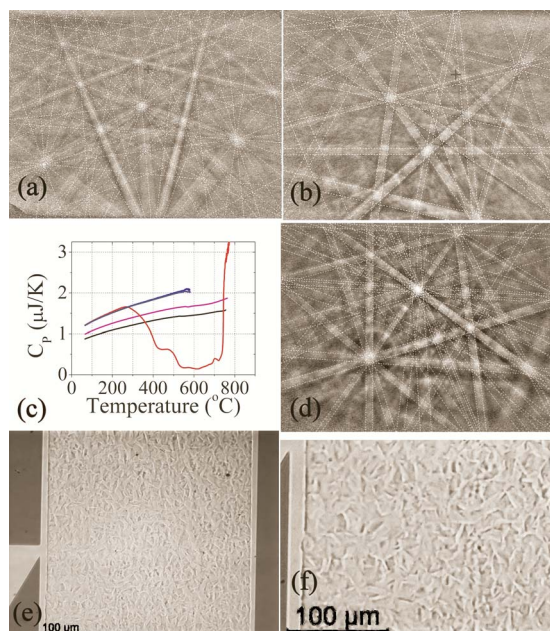


FIG. 2. (Color online) (a) Indexed EBSD pattern corresponding to the  $\theta$ -Ni<sub>2</sub>Si phase found in the sample heated to 850 °C. (b) Indexed EBSD pattern of the NiSi phase found in sample heated to 850 °C. (c) Heat capacity results from a sample that was heated to a lower temperature (790 °C in the first pulse) and (d) the indexed EBSD pattern of the end product (NiSi) of this experiment. (e), (f) Grain structure of the reaction products of sample heated to 850 °C.

tions and make quantitative heat capacity and enthalpy measurements of solid state reactions even in cases where complex phase changes occur.

Supported by NIST under NIST-70NANB7H6162, NIST-70NANB5H1162 and by the NSF under NSF-ECS-0622117, DMR-0108694 and NSF-DMR-0735286. Research carried out at the UIUC MRL, Cornell University NanoScale Facility, and NIST Center for Nanoscale Science and Technology. We thank D.A. Jeffers at UIUC MRL for assistance with RBS measurements. The full description of the software and databases used in this paper requires the identification of certain software and databases. The inclusion of such infor-

mation should in no way be construed as indicating that such software or databases are endorsed or recommended by NIST or that it is necessarily the best software or database for the purposes described.

- <sup>1</sup>J. A. Kittl, M. A. Pawlak, C. Torregiani, A. Lauwers, C. Demeurisse, C. Vrancken, P. P. Absil, S. Biesemans, C. Coia, C. Detavernier, J. Jordan-Sweet, and C. Lavoie, *Appl. Phys. Lett.* **91**, 172108 (2007).
- <sup>2</sup>C. Detavernier, A. S. Ozcan, J. Jordan-Sweet, E. A. Stach, J. Tersoff, F. M. Ross, and C. Lavoie, *Nature (London)* **426**, 641 (2003).
- <sup>3</sup>S. Abhaya, G. Amarendra, S. Kalavathi, P. Gopalan, M. Kamruddin, A. K. Tyagi, V. S. Sastry, and C. S. Sundar, *Appl. Surf. Sci.* **253**, 3799 (2007).
- <sup>4</sup>L. W. Cheng, H. M. Lo, S. L. Cheng, L. J. Chen, and C. J. Tsai, *Mater. Sci. Eng., A* **409**, 217 (2005).
- <sup>5</sup>D. Z. Chi, R. T. P. Lee, and A. S. W. Wong, *Thin Solid Films* **515**, 8102 (2007).
- <sup>6</sup>A. Alberti, C. Bongiorno, E. Rimini, and M. G. Grimaldi, *Appl. Phys. Lett.* **89**, 102105 (2006).
- <sup>7</sup>K. Tsutsui, R. Xiang, K. Nagahiro, T. Shiozawa, P. Ahmet, Y. Okuno, M. Matsumoto, M. Kubota, K. Kakushima, and H. Iwai, *Microelectron. Eng.* **85**, 315 (2008).
- <sup>8</sup>M. Bhaskaran, S. Sriram, J. D. Plessis, and A. S. Holland, *Electron. Lett.* **43**, 479 (2007).
- <sup>9</sup>G. Majni, M. Costato, and F. Panini, *Thin Solid Films* **125**, 71 (1985).
- <sup>10</sup>K. De Keyser, C. Detavernier, and R. L. Van Meirhaeghe, *Appl. Phys. Lett.* **90**, 121920 (2007).
- <sup>11</sup>K. De Keyser, C. Van Bockstael, C. Detavernier, R. L. Van Meirhaeghe, J. Jordan-Sweet, and C. Lavoie, *Electrochem. Solid-State Lett.* **11**, H266 (2008).
- <sup>12</sup>M. Y. Efremov, E. A. Olson, M. Zhang, S. L. Lai, F. Schiettekatte, Z. S. Zhang, and L. H. Allen, *Thermochim. Acta* **412**, 13 (2004).
- <sup>13</sup>M. Y. Efremov, F. Schiettekatte, M. Zhang, E. A. Olson, A. T. Kwan, R. S. Berry, and L. H. Allen, *Phys. Rev. Lett.* **85**, 3560 (2000).
- <sup>14</sup>M. Y. Efremov, E. A. Olson, M. Zhang, Z. Zhang, and L. H. Allen, *Phys. Rev. Lett.* **91**, 085703 (2003); L. Hu, Z. Zhang, M. Zhang, M. Y. Efremov, E. A. Olson, L. P. de la Rama, R. K. Kummamuru, and L. H. Allen, *Langmuir* **25**, 9585 (2009).
- <sup>15</sup>S. L. Lai, J. R. A. Carlsson, and L. H. Allen, *Appl. Phys. Lett.* **72**, 1098 (1998).
- <sup>16</sup>E. A. Olson, M. Yu Efremov, M. Zhang, Z. Zhang, and L. H. Allen, *J. Appl. Phys.* **97**, 034304 (2005).
- <sup>17</sup>D.-C. Kim, T. G. Lee, and Y.-H. Kim, *J. Mater. Sci. Mater. Electron.* **10**, 85 (1999).
- <sup>18</sup>R. K. Kummamuru, L. Hu, L. Cook, M. Y. Efremov, E. A. Olson, and L. H. Allen, *J. Micromech. Microeng.* **18**, 095027 (2008).
- <sup>19</sup>P. Nash and A. Nash, *Bull. Alloy Phase Diagrams* **8**, 6 (1987).
- <sup>20</sup>M. E. Schlesinger, *Chem. Rev. (Washington, D.C.)* **90**, 607 (1990).
- <sup>21</sup>K. Toman, *Acta Crystallogr.* **5**, 329 (1952).